Refined X-ray Structures of the Oxidized, at 1.3 Å, and Reduced, at 1.17 Å, [2Fe−2S] Ferredoxin from the Cyanobacterium *Anabaena* PCC7119 Show Redox-Linked Conformational Changes†

Renaud Morales,‡ Marie-Hélène Chron,‡ Gilbert Hudry-Clergeon,§ Yves Pétillot,|| Sofie Norager,‡,⊥ Milagros Medina,○ and Michel Frey*,‡

Laboratoire de Cristallographie et de Cristallogénèse des Protéines, Laboratoire d'Enzymologie Moléculaire, and Laboratoire de Spectrométrie de Masse, Institut de Biologie Structurale J.P. Ebel, CEA-CNRS, 41 rue Jules Horowitz, F38027 Grenoble, France, and Departamento de Bioquímica y Biología Molecular y Celular, Facultad de Ciencias, Universidad de Zaragoza, 50009-Zaragoza, Spain

Received July 8, 1999; Revised Manuscript Received September 21, 1999

ABSTRACT: The chemical sequence of the [2Fe−2S] ferredoxin from the cyanobacterium *Anabaena* PCC7119 (Fd7119) and its high-resolution X-ray structures in the oxidized and reduced states have been determined. The Fd7119 sequence is identical to that of the ferredoxin from the PCC7120 strain (Fd7120). X-ray diffraction data were collected at 100 K with an oxidized trigonal Fd7119 crystal, at 1.3 Å resolution, and with an orthorhombic crystal, previously reduced with dithionite and flash frozen under anaerobic conditions, at 1.17 Å resolution. The two molecular models were determined by molecular replacement with the [2Fe−2S] ferredoxin from the strain PCC7120 (Rypniewski, W. R., Breiter, D. R., Benning, M. M., Wesenberg, G., Oh, B.-H., Markley, J. L., Rayment, I., and Holden, H. M. (1991) *Biochemistry 30*, 4126−4131.) The final *R*-factors are 0.140 (for the reduced crystal) and 0.138 (for the oxidized crystal). The [2Fe−2S] cluster appears as a significantly distorted lozenge in the reduced and oxidized redox states. The major conformational difference between the two redox forms concerns the peptide bond linking Cys46 and Ser47 which points its carbonyl oxygen away from the [2Fe−2S] cluster ("CO out") in the reduced molecule and toward it ("CO in") in the oxidized one. The "CO out" conformation could be the signature of the reduction of the iron atom Fe1, which is close to the molecular surface. Superposition of the three crystallographically independent molecules shows that the putative recognition site with the physiological partner (FNR) involves charged, hydrophobic residues and invariant water molecules.

Ferredoxins are iron−sulfur proteins that are found in bacteria, plants, and mammals where they are mainly involved in many electron transfer reactions. They are structurally characterized by the presence of one or several clusters, [2Fe−2S], [3Fe−4S], or [4Fe−4S] and have been subjected for many years to a wealth of physicochemical and biological studies (*1*, *2*, *3*).

In plants, algae or photosynthetic bacteria [2Fe−2S] ferredoxins mediate the transfer of two electrons, in two successive one electron steps, from photosystem I to Ferredoxin-$NADP^+$-oxidoreductases (FNR), which, as the name indicates, eventually reduce $NADP^+$ following the reaction $NADP^+ + 2e^- + H^+ \rightleftharpoons NADPH$ (*4*). Moreover, electron transfer between ferredoxin and FNR involves the formation of a complex (*5*, *6*).

To elucidate the mechanisms of electron or hydride transfers, kinetic, thermodynamic, and biological studies of the FNR/ferredoxin system from Spinach (e.g., *7*, *8*) and *Anabaena* have been pursued (e.g., *9*, *10*).

Along these lines, the crystal structures of the [2Fe−2S] wild-type ferredoxin *Anabaena* PCC7120 (Fd7120) (*11*) and six mutants (*9*) have been determined by X-ray diffraction, at resolutions ranging from 2.5 to 1.7 Å as well as the crystal structures of *Anabaena* PCC7119 FNR and of a complex FNR-$NADP^+$ (*12*), at 1.8 and 2.25 Å resolution, respectively.

Moreover, the crystal structures of several plant-type [2Fe−2S] ferredoxins, all in their oxidized state, have already been determined on the basis of X-ray diffraction data obtained at resolutions ranging from 2.5 to 1.7 Å. They show remarkably similar main chain folds and their [2Fe−2S] cluster geometries are very close to each other (*9*, *11*, *13*, *14*, *15*, *16*, *17*, *18*). More recently, the coordinates of the oxidized *Chlorella fusca* [2Fe−2S] ferredoxin, obtained with 1.4 Å X-ray data have been deposited at the Protein data bank (1AWD). Furthermore, several possible models of interactions with their physiological partners have been proposed and discussed on the basis of X-ray structures and electrostatic potential analysis (e.g., *16*, *19*, *20*).

‡ Laboratoire de Cristallographie et de Cristallogénèse des Protéines.
§ Laboratoire d'Enzymologie Moléculaire.
|| Laboratoire de Spectrométrie de Masse.
○ Departamento de Bioquímica y Biología Molecular y Celular.
⊥ Present address: Centre for Crystallographic Studies, Department of Chemistry, University of Copenhagen, Universiteitsparken 5, DK-2100 Copenhagen, Denmark.
* Corresponding author. Telephone: 33 4 76 88 59 24. Fax: 33 4 76 88 51 22. E-mail: frey@lccp.ibs.fr.
† This work was supported by the CEA, the CNRS, and the Ministère de l'Education Nationale, de la Recherche et de la Technologie.
[1] Abbreviations: FNR, ferredoxin-$NADP^+$ reductase; Fd, ferredoxin; Fd7119, ferredoxin from *Anabaena* PCC7119; Fd7120, ferredoxin from *Anabaena* PCC7120; *red*, reduced; *ox*, oxidized; PDB, Protein Data Bank.

10.1021/bi991578s CCC: $18.00
Published on Web 11/09/1999

Table 1: Mass Analysis (ESMS) of Fd7120 and Fd7119[a]

	expected mass Fd7120 (sequence)	measured mass Fd7120	measured mass Fd7119
native uncleaved proteins	10698.73 (A1-Y98)	10298.4	10698.3
cleaved carboxy-methylated proteins			
fragment 1	465.56 (A1-K4)	465.3	465.4
fragment 2	1174.33 (V5−K15)	1174.2	1174.0
fragment 3	4178.47 (H16−K52)	4178.4	4178.6
fragment 4	4516.92 (L53-K93)	unobserved	unobserved
fragment 5	667.68 (E94-Y98)	unobserved	unobserved
fragment 4 + 5	5166.58 (L53-Y98)	5167.2	5166.8

Fd7120 sequence (*11*)

10 20 30 40 50

ATF**K**VTLINEAEGT**K**HEIEVPDDEYILDAAEEQGYDLPFSCRAGACSTCAG**K**LV

60 70 80 90

SGTVDQSDQSFLDDDQIEAGYVLTCVAYPTSDVVIQTHKEEDLY

[a] The masses of the uncleaved apoproteins and the masses of the four fragments obtained after lysine-endopeptidase cleavage of the carboxymethylated protein were compared. No cleavage was observed at K93, probably due to high acidic environment. The known sequence of Fd7120 is indicated. The 21 corresponding amino acid residues sequenced by Edman degradation in Fd7119 are underlined. Lysyl residues cleaved by the lysine-endopeptidase are indicated in bold.

Recently, we have obtained large crystals of the [2Fe−2S] ferredoxin from *Anabaena* PCC7119 (Fd7119) diffracting at atomic resolution. This prompted us to determine its chemical sequence and refine crystallographic models in the oxidized and reduced states to obtain an accurate geometry of the [2Fe−2S] cluster and its environment in both redox states. Here, we report a structural analysis derived from X-ray diffraction data collected at 1.3 Å resolution with a Fd7119 oxidized crystal and at 1.17 Å with a partially reduced crystal. This allowed, in particular, significant comparisons with [2Fe−2S] containing model compounds and gave insights on the role of the protein matrix (*21*).The structure of the molecular surface close to the cluster, which is thought to be involved in the recognition of FNR and thus in intermolecular electron-transfer process, has also been analyzed. Finally, the present paper constitutes, at our knowledge, the first report on a three-dimensional atomic structure of a reduced plant-type [2Fe−2S] ferredoxin.

EXPERIMENTAL PROCEDURES

Purification and Biochemical Characterization. Anabaena PCC7119 ferredoxin (Fd7119) was isolated and purified as previously described (*22*). The unknown sequence of Fd7119 was studied by Edman degradation and electrospray mass spectrometry (ESMS) and compared to that of the *Anabaena* PCC7120 ferredoxin (Fd7120).

Automated Edman degradation was performed with an Applied Biosystems gas-phase Sequencer model 477A with on-line analysis of the phenylthiohydanthoin derivatives at 260 nm.

Cysteines of both ferredoxin Fd7119 and Fd7120 were carboxymethylated using sodium iodoacetate (70 mM) at pH 6.5 in 6 M guanidine·HCl. Carboxymethylated proteins were cleaved by lysine-endopeptidase. Digestions were performed at an enzyme/substrate ratio of 1:20 (by mass) for 5 h at 37 °C.

Purification of proteins or peptides generated by enzymatic cleavage was carried out by reverse phase HPLC, using an Applied Biosystems Model 130A system equipped with a C8 column (Aquapore RP-300, 100 mm × 2.1 mm). The column was equilibrated with solvent A (trifluoroacetic acid 0.1%, v/v, in water) and a linear gradient from 25 to 65% of solvent B (CH3CN/trifluoroacetic acid 70:0.085%, v/v, in water) was performed over 50 min with a flow rate of 200 μL/min.

ESMS analyses were carried out on a Sciex (Thornhill) API/III triple quadrupole mass spectrometer equipped with an atmospheric pressure ionization source. The ionspray needle voltage was maintained at 5 kV. Each mass spectrum was an average of four scans. The samples were infused into the source at a concentration of about 0.5 mg/mL in 25% MeOH/1% AcOH (v/v).

The results of these biochemical characterizations are summarized in Table 1.

Crystallization. Crystals of Fd7119 were obtained at 4 °C and pH 5.5 by the "hanging drop" vapor diffusion method under conditions similar to those of Fd7120 (*11*), except that sodium succinate was used instead of potassium succinate. Crystals of about 0.5 × 0.5 × 0.5 mm^3 grew within 2 days. Like for Fd7120, two crystal forms are often present within the same drop (*9*): one is orthorhombic (a = 37.22 Å, b = 37.37 Å, c = 146.6 Å, $\alpha = \beta = \gamma = 90$ deg; S. G. $P2_12_12_1$ and two molecules, mol-1 and mol-2 per asymmetric unit) and the other trigonal ($a = b$ = 37.4 Å, c = 145.5 Å, $\alpha = \beta = 90$ deg, $\gamma = 120$ deg; S.G $P3_221$ and one molecule per asymmetric unit).

To obtain the structure of the oxidized Fd7119 ferredoxin, a trigonal crystal, grown in aerobic conditions at 4 °C, was dipped for a few seconds into a cryoprotectant solution containing 20% glycerol and 80% crystallization reservoir buffer and flash-frozen in liquid propane (123 K).

To prepare the reduced Fd7119 crystal, we first checked the reducing conditions with ferredoxin in the crystallization medium. This sample was introduced in a glovebox under anaerobic conditions (about 1 ppm oxygen) and 1 mM dithionite was added to it. Spectrophotometric measurements were then performed in an airtight cell. The spectrum showed that the ferredoxin was reduced. As a further check, we left the solution exposed to air and measured again its optical absorbance.

The diffusion rate of the reducing agent into the crystal solvent channels was expected to be lower than in solution.

Table 2: Crystallographic Data Collection and Processing[a]

	reduced crystal	oxidized crystal
space group	$P2_12_12_1$	$P3_221$
a (Å)	37.22	37.4
b (Å)	37.37	37.4
c (Å)	146.6	135.5
resolution range (Å)	30.0−1.17	30−1.3
unique reflections	67 611	27 431
redundancy	4.3 (2.8)[a]	6.5 (3.3)[a]
completeness (%)	95.5 (89.3)[a]	96.5 (80.5)[a]
R_{sym} (%)[b]	3.7 (11.1)[a]	6.1 (22.6)[a]
$\langle I\rangle/\langle\sigma I\rangle$ overall	12.0 (6.1)[a]	5.8 (3.0)[a]

[a] Numbers in parentheses correspond to the data in the last resolution shell, 1.22−1.17 Å and 1.34−1.28 Å for the reduced and oxidized crystal, respectively. [b] $R_{sym} = \sum|I_i - \langle I\rangle|/\sum I_i$; I_i is the intensity of the *i*th observation and $\langle I_i\rangle$ is the mean intensity of the reflection.

However, the soaking time in the reduced crystallization solution was necessarily limited, because during the experiment, we had to keep the crystal on ice at its crystallization temperature (4 °C vs about 20 °C for the glovebox). Therefore, to obtain a reduced crystal, we transferred an orthorhombic sample on ice into the glovebox and soaked it, between 30 min and 1 h, in the crystallization solution to which 10 mM (vs 1 mM in solution) sodium dithionite and 20% (v/v) glycerol were added (*23*). Then the crystal was picked up with a loop from the solution, flash-cooled and kept in liquid propane before being removed from the glovebox. All solutions had previously been deoxygenated, by bubbling gaseous nitrogen for about 15 min in the glovebox.

X-ray Data Collection and Processing. During X-ray data collection, the oxidized and reduced frozen crystals were respectively kept within a nitrogen stream at 100 K. For the oxidized crystal, we used the European Synchrotron (ESRF) beamline BM2 with a CCD (XRII−CCD) detector ($\lambda = 0.98$ Å). For the reduced crystal, we used the ESRF beam line BM14 with a MAR research 345 image plate detector ($\lambda = 0.751$ Å) (Table 2). In both cases, two sets of images, one at high resolution (8−1.15 Å) and one at a medium resolution (30−2.1 Å), were recorded. The data were processed with XDS (version 93) (*24*) for the oxidized crystal and MOSFLM (version 5.5) (*25*) for the reduced one. All data were finally scaled with the CCP4 program SCALA (*26*) (Table 2).

Refinement. We generated two initial atomic models using X-ray data, between 15 and 2.5 Å, of the oxidized and reduced crystal, respectively, and the structure of Fd7120 (*11*) (Protein Data Bank ID: 1FXA). The molecules, excluding waters, were placed in their corresponding crystal cells, by molecular replacement and fast rigid body refinement, by the AMoRe program package (*27*). The initial crystallographic *R*-factors were in each case about 0.43.

Several interleaving cycles of manual model building of the polypeptide chain with O (*28*) and isotropic refinement with the program REFMAC (*29*) coupled with automatic addition of solvent water atoms by ARP (*30*) were then carried out, including progressively high-resolution X-ray data. Features of positive density greater than 3σ in $F_o - F_c$ difference Fourier maps were modeled as the oxygen atom of a water molecule or alternate conformations for several side chains. At this stage of the refinement, an alternate conformation of the 46−47 peptide was also observed in the reduced crystal but not modeled. The resulting R- and

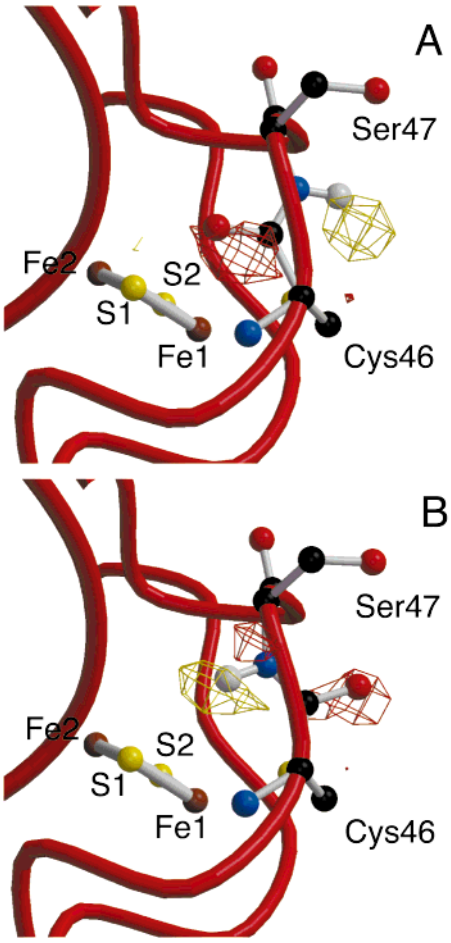

FIGURE 1: The two alternate conformations of the Cys46-Ser47 peptide and its environment in the reduced crystal with CO pointing (A) toward the cluster S2 sulfur atom ("CO in") and (B) away from it ("CO out"). Electron density maps were computed with amplitudes ($|F_o| - F_c|$). For each conformation, $|F_c|$ and phases were calculated with a refined model from which the other conformation has been omitted. Positive and negative difference electron density contoured at 3σ are drawn in yellow and red, respectively. Carbon atoms are colored in black, nitrogen in blue, oxygen in red, hydrogen in white, sulfur in yellow, and iron in brown. The figure was drawn with BobScript (*51*).

R_{free}-factors were 0.19 and 0.235, respectively for the reduced crystal and 0.17 and 0.215 for the oxidized one.

We completed the refinements of the oxidized and reduced structures using the program SHELXL-97 (*31*) with F^2 as observables excluding resolution data at resolution lower than 15.0 Å but without applying any sigma cutoff. Conjugate gradient option was used and protein bond and angle restraints were applied (*32*) with the default values proposed by SHELX-97 for weights. No stereochemical restraints were applied on the [2Fe−2S] cluster iron and sulfur atoms. Here again, we manually adjusted the polypeptide chain through several interleaving graphic sessions.

For the reduced crystal, difference Fourier maps confirmed the presence of main chain alternate conformations centered at the 46−47 peptide. One of this conformation shows the Cys46-CO pointing toward the cluster ("CO in") as in the oxidized crystals, whereas the other one has the Cys46-CO pointing away from the cluster ("CO out") (Figure 1). Examination of the temperature factors of the average structure indicated more precisely that these conformational changes occurred at the main chain segment including Ala45

Table 3: Refinement by SHELX-97 with Anisotropic Temperature Factors[a]

	reduced crystal mol-1, mol-2	oxidized crystal
resolution range (Å)	15.0−1.17	15.0−1.3
reflections used	67 145	26 254
atomic parameters	17 225	8098
restraints	21 431	9598
hydrogens	8944	3876
solvent molecules	369	238
heteroatoms	8	4
R_{work} (%)[a]	14.00	13.77
R_{free} (%)[a]	18.37	19.14
Goodness of fit[b]	3.5	2.005
wR2 (F2)[c]	34.28	32.94
average *B*-factor		
protein (Å^2)	17.16, 20.3	12.5
cluster (Å^2)	11.5, 13.6	9.4
solvent (Å^2)	36.0	33.6
rms deviations		
bond length (Å)	0.013	0.017
bond angles (deg)	0.029	0.034

[a] Rfactor $= \sum|F_o - F_c|/\sum F_o$ [b] Goodness of fit $=\{\sum[w(F_o^2 - F_c^2)^2]/(n-p)\}^{1/2}$; n = reflections, p = refined parameters. [c] wR2 $= \{\sum w(F_o^2 - F_c^2)^2/\sum[w(F_o^2)^2]\}^{1/2}$.

to Thr48, the cluster atoms Fe1 and S2 and to a lesser extent the side chains Ala45, Cys46, Ser47, and Thr48. When we refined one of the two conformers, new $F_o - F_c$ difference maps clearly revealed the electron density of the alternate Cys46-CO conformation and vice-versa (Figure 1). It has not been possible to refine separately the Fe1 and S2 alternate positions. Therefore, only the two conformers of the polypeptide chain Ala45 to Thr48 segment were included in the model and refined for several cycles constraining the sum of their respective occupancies to unity. The occupancy of the ("CO in") conformation was for the *two* crystallographically independent molecules, mol-1 and mol-2, 0.60 and 0.45, respectively. As a final check, we verified that the resulting $F_o - F_c$ difference map was devoid of any significant feature.

The contribution of the solvent continuum was taken into account by the SHELXL SWAT instruction. In the last stages, the analysis of the electron density maps suggested that thermal parameters of many atoms could be modeled as anisotropic. The validity of this assumption was confirmed, when applied, by a further decrease of the R_{free}-factor by 0.025. Moreover, since many hydrogen atoms were clearly "visible" on $F_o - F_c$ difference electron density maps, they were included in the final stage of the refinement resulting in a further 0.01 decrease in R_{free}. No significant feature has been observed on the final $F_o - F_c$ difference electron density maps. The final R, R_{free} and wR2 factor (based on the F2 factors) are 0.14, 0.184, and 0.34 respectively for the reduced orthorhombic crystal and 0.138, 0.191, and 0.33 for the oxidized trigonal crystal. The statistics of the respective refinements are described in Table 3. All X-ray data were included in these final calculations.

It should be also emphasized that during the final stages of the refinement the iron and sulfur atoms were refined with SHELXL without any restraint. Moreover the errors on the atomic parameters were estimated from inversion of the block least-squares matrix with two blocks, overlapping each other by three residues, for each molecule and an additional block for water molecules.

Superposition of [2Fe−2S] Containing Proteins. To compare the [2Fe−2S] environments in [2Fe−2S] containing proteins, we simply fitted by least-squares the Cα atoms of the four liganding cysteines. The data have been retrieved from the Protein Data Bank (http://www.rcsb.org/pdb/) and the Prosthetic Groups and Metal Ions in Protein Active Sites Database Version 2.0 (PROMISE) at the University of Leeds (http://bmbsgi11.leeds.ac.uk/promise/).

RESULTS

Biochemical Properties. N-terminal sequencing showed that the first 21 residues of Fd7119 are identical to the first 21 residues of Fd7120 (Table 1). Moreover, the two apoproteins are eluted at the same place by reverse-phase chromatography and yield the same number of enzymatic peptides, eluting at the same place with the same relative intensity (not shown). Analyses by mass spectroscopy of apoproteins or carboxymethylated fragments gives, for Fd7119 and Fd7120, identical mass values (Table 1), which is in total agreement with the theoretical values expected for Fd7120. Therefore, except for a possible substitution by a residue with same mass and similar hydrophobicity (e.g., Leu/Ile), the biochemical analyses strongly suggested that the chemical sequence of the [2Fe−2S] ferredoxin from the strain PCC7119 is identical to that from the strain PCC7120. As we will see below, this is in accordance with the crystallographic analysis.

Reduction of the Orthorhombic Crystal. After reduction of the ferredoxin solution in crystallization condition the UV−visible spectrum showed an important decrease of the peak absorbance at λ = 330, 420, and 460 nm, which identifies a reduced [2Fe−2S] cluster. Since subsequent reoxidation led to a spectrum similar to that of an oxidized solution, we inferred that Fd7119 could be reduced at pH 5.5 by dithionite in its crystallization solution. Unfortunately, it has not been possible to obtain an interpretable optical spectrum for the crystal after reduction, due to the low absorbance.

Quality of the X-ray Diffraction Data and Refined Models. Because of the quality and size of the crystals and the use of cryogenic techniques coupled with synchrotron radiation (brillancy and high energy radiation) X-ray data are of good quality as shown by low R_{merge}-factors, rather high $\langle I\rangle/\langle\sigma I\rangle$ and redundancy (Table 2). This in turn accounts for the high quality of the final electron density map (Figure 2) and consequently for the accuracy and precision of the three atomic models. Moreover, the overall correlation between the observed and calculated electron densities is over 0.9, which confirms that the total Fd7119 chemical sequence is identical to that of Fd7120.

Overall Folding. Not surprisingly, Fd7119 is roughly globular and the folding of its polypeptide chain is very similar to that of plant-type ferredoxin of known crystal structure including Fd7120 (*9*, *11*). Its most salient features consist of a four stranded β-pleated sheet opposite to the protruding zone, containing the cluster, two α-helices, and the cluster liganding peptides. The [2Fe−2S] cluster, close to the molecular surface, is coordinated through the iron atoms to four cysteine sulfur atoms (Figure 3). The folds of the three crystallographically independent molecules (one in the oxidized crystal and two in the reduced crystal) are very

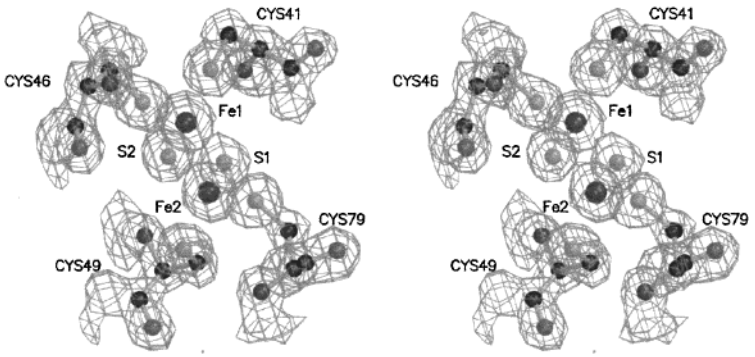

FIGURE 2: Stereoview of the refined model and electron density $2|F_o| - |F_c|$ map (contoured at 1σ) of the [2Fe−2S] cluster and its four cysteine ligands. Carbon atoms are colored in black, nitrogen in blue, oxygen in red, sulfur in yellow, and iron in brown. The figure was drawn with BobScript (51).

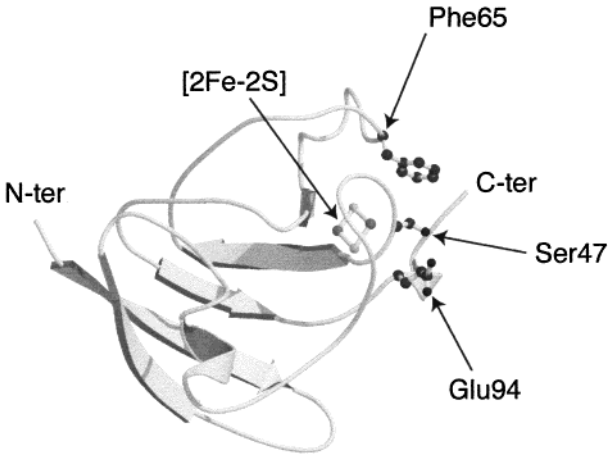

FIGURE 3: Ribbon diagram depicting the three-dimensional structure of *Anabaena PCC7119* ferredoxin. The [2Fe−2S] cluster and three residues (Phe65, Ser47, and Glu94) known by site directed mutagenesis to be important for electron transfer to FNR (*9*) are represented. The figure was drawn with MolScript (*52*).

close to each other since the radial mean square deviations (rms) between molecules range from about 0.3 Å for the Cα chain to about 0.9 Å for all the atoms excluding conformational differences between some surface side chains.

Terminal Tyr98 Conformation. In the trigonal crystal, Tyr98 is pointing into the solvent and is stabilized by an hydrogen bond and contacts with symmetry related molecules, which accounts for the very well-defined corresponding electron density. In the orthorhombic crystal, Tyr98 is pointing toward Ser47 and Glu94 in both mol-1 and mol-2, In mol-2 Tyr98-Oη is making a strong hydrogen bond (2.8 Å) with Ser47-Oγ and a close contact (3.2 Å) with Phe65-Cζ. The latter contact is obviously too short. This is most probably due to some crystallographic disorder reflected by a relatively weak electron density for both mol-1 and mol-2. This point is discussed below.

Alternate Conformations in the Reduced Crystal. The major difference between the oxidized and reduced crystal concerns the peptide linking Cys46 and Ser47. In the oxidized crystals, the Cys46 carbonyl oxygen atoms is always pointing toward the cluster ("CO in"). In the *two* crystallographically independent molecules, mol-1 and mol-2, present in the reduced crystal, the 46−47 peptide can adopt two conformations with the Cys46 carbonyl oxygen pointing either toward the cluster S2 atom like in the oxidized crystal ("CO in") or away from it ("CO out") (see Table 4). This 46−47 peptide flip is associated with conformational changes of neighboring residues as revealed by their relatively higher B factors in the average structure. Some minor positional changes of Fe1, S2 and Cys46-Sγ are also probably taking place in view first of their relatively higher temperature factors (about 15 $Å^2$ vs 12 A^2 for the neighboring atoms). Along these same lines, it is of interest to note that the ellipsoids representing the cluster atoms anisotropic temperature factors are elongated along a direction that is nearly perpendicular to the cluster distorted plane; the most elongated ones being those of Fe1 and S2. However, as mentioned above, it has not been possible to refine separately the Fe1 and S2 alternate positions. It follows that the [2Fe−2S] cluster geometry, as we see it in the reduced crystal, has to be considered as an average between two slightly different conformations.

Geometry of the [2Fe2S] Cluster and its Environment. Whatever the crystal redox state, the [2Fe−2S] cluster appears as a nonplanar distorted lozenge. The angles between the normals to the S1−Fe1−S2 (close to the molecular surface) and S1−Fe2−S2 (buried) moieties are 6.8 deg in the oxidized crystal and 8.8 deg for mol-1 and 8.7 deg for mol-2 in the reduced one. On the whole, the Fe1−S1, Fe1−Sγ, and Fe1−S2 distances are both significantly longer and more widely distributed than the Fe2−S1, Fe2−Sγ, and Fe2−S2 distances. By contrast, the Fe1−Fe2 distances are remarkably constant (average = 2.747 ± 0.002 Å (Table 4).

NH···S Hydrogen Bonds. The cysteine ligands and the sulfur atoms of the [2Fe−2S] cluster are involved in a network of hydrogen bonds with main chain peptide nitrogen atoms (Figure 4). As in plant-type ferredoxins (*13*) the NH···S bonds involving the S1−Fe1−S2 moiety outnumber by far those involving the S1−Fe2−S2 moiety. Moreover, in the reduced crystal, the "CO out" alternate conformation of the Cys46−Ser47 peptide bond corresponds to an additional NH···S bond with S2, again on the side of the cluster S1−Fe1−S2 moiety (Table 5).

OH···O Surface Hydrogen Bonds. The hydrogen bond between Ser47-Oγ and Glu94-$O_{\epsilon 2}$ is particularly important, since site-directed mutagenenesis experiments have shown that its absence could block the electron-transfer pathway out of the ferredoxin molecule and perturb the formation of a productive complex between Fd and FNR (*9*). This bond is quite short in the oxidized crystal (O···O = 2.51 Å; Figure 5). In the reduced crystals, the same bond can also be inferred

Table 4: [2Fe−2S] Cluster Geometry in Reduced Crystal (1.17 Å), Oxidized Crystal (1.3 Å), and Model Compounds[a]

	reduced crystal		oxidized	$[FeS(SCH_2)_2C_6H_4]_2^{2-}$/	$(Net_4)_2[Fe_2S_2\{S\text{-}2,6\text{-}$
	mol-1	mol-2	crystal	$[Fe_2S_2(SC_6H_4CH_3)_4]^2$	$(t\text{−}Bu\ CONH)2C_6H_3\}_4]$
bonds (Å)					
Fe1−Fe2	2.749 (4)	2.747 (4)	2.746 (5)	2.698 (1)/2.691 (1)	2.671 (6)
Fe1−S1	2.293 (5)	2.285 (5)	2.278 (7)		
−S2	2.261 (5)	2.233 (5)	2.234 (7)		
−41Sγ	2.328 (4)	2.361 (6)	2.335 (7)		
−46Sγin	2.299 (50)	2.192 (40)	2.276 (7)		
−46Sγout	2.328 (40)	2.300 (30)			
Fe2−S1	2.235 (5)	2.218 (4)	2.227 (7)	2.232 (2)/2.202 (1)	2.203 (7)
−S2	2.178 (5)	2.197 (5)	2.184 (7)	2.185 (1/2.200 (1)	2.198 (7)
−49Sγ	2.299 (4)	2.313 (6)	2.287 (7)	2.300 (2)/2.312 (1)	2.308 (8)
−79Sγ	2.301 (5)	2.297 (5)	2.288 (7)	2.300 (2)/2.312 (1)	2.328 (7)
angles (deg)					
S1−Fe1−S2	101.8 (2)	102.2 (2)	102.2 (3)	104.73 (5)/104.61 (4)	
S1−Fe1−46Sγin	111.3 (7)	112.8 (6)	108.1 (2)		
S1−Fe1−46Sγout	108.9 (8)	110.8 (6)			
S1−Fe1−41Sγ	119.2 (2)	119.3 (2)	119.8 (2)		
S2−Fe1−41Sγ	102.9 (2)	103.2 (2)	102.3 (3)		
S2−Fe1−46Sγin	116.7 (8)	114.9 (6)	119.1 (3)		
S2−Fe1−46Sγout	119.7 (8)	118.5 (6)			
41Sγ-Fe1−46Sγin	105.1 (8)	104.5 (8)	106.0 (3)		
41Sγ-Fe1−46Sγout	104.9 (8)	103.2 (8)			
Fe1−S1−Fe2	74.7 (2)	75.2 (2)	75.1 (2)	75.27 (5)/75.39 (4)	
Fe1−S2−Fe2	76.5 (2)	76.6 (2)	76.8 (3)		
S1−Fe2−S2	106.4 (2)	105.5 (2)	105.6 (3)	104.73 (5)/104.61(4)	
S1−Fe2−49Sγ	113.0 (2)	114.3 (2)	112.3 (3)	112.33 (5)/114.48 (4)	
S1−Fe2−79Sγ	115.2 (2)	114.9 (2)	116.0 (3)	110.78 (5)/105.32 (4)	
S2−Fe2−79Sγ	106.0 (2)	105.6 (2)	105.0 (3)	112.05 (5)/105.48 (4)	
S2−Fe2−49Sγ	110.7 (2)	111.4 (2)	111.2 (3)	110.66 (5)/115.81 (4)	
49Sγ-Fe2−79Sγ	105.2 (2)	104.9 (2)	106.6 (3)		

[a] Numbers in parentheses correspond to the last digit standard uncertainties; in = Cys46-CO pointing toward the cluster, out = Cys46-CO pointing away from the cluster.

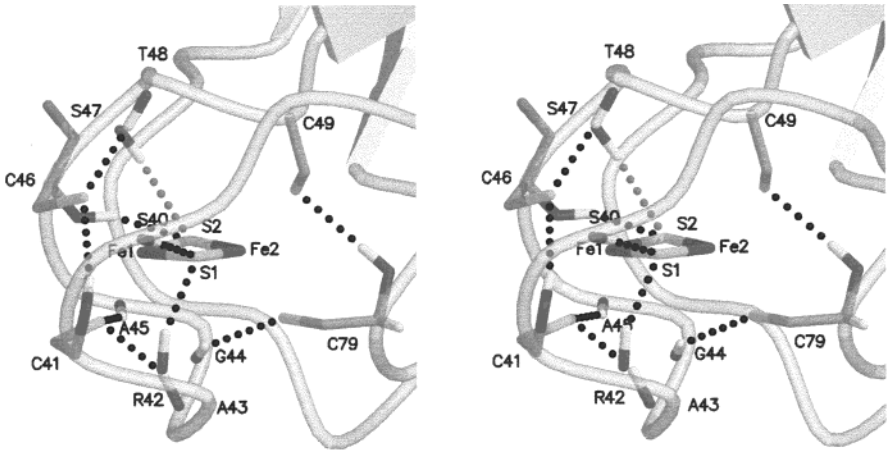

FIGURE 4: Stereoview of the hydrogen bond (NH···S) network involving cluster and cysteine ligands sulfur atoms in the reduced crystal ("CO out" conformation). The additional Ser47NH···S2 bond is represented by red dashed line and the other ones by black dashed lines. Carbon atoms are colored in gray. The figure was drawn with MolScript (*52*).

as the Ser47 and Glu94 electron density maps are reasonably well-defined in mol-1 and mol-2. However, due to the limits of the refinement of the alternate conformation, the discrepancies between O···O equivalent hydrogen bonds are quite large (2.77 Å (mol-1) and 3.32 Å (mol-2) for the "CO in" and 2.49 Å (mol-1) and 2.92 Å (mol-2) for the "CO out" one). Therefore, it is not possible to conclude if the conformational change involves a significant modification to the geometry of this critical hydrogen bond. Moreover, a very strong hydrogen bond between two surface residues Glu32 and Glu24 is also visible in the oxidized (O···O = 2.59 Å) and in the reduced crystals (O···O = 2.56 Å).

DISCUSSION

Does the Reduced Crystal Contain Reduced Ferredoxin Molecules? About half of the molecules present in the reduced crystal show their Cys46 peptide carbonyl oxygen pointing away from the cluster S2 atom ("CO out") and not toward it ("CO in") like in the oxidized crystals. Since this solvent exposed oxygen is not involved in any crystal packing interaction, this suggested that the "flip" of the Cys46 negatively charged peptide carbonyl might be characteristic of the reduced protein.

^{57}Fe Mössbauer spectroscopy has shown that the [2Fe−2S] cluster contains two ferric Fe^{3+} in the oxidized state and

Table 5: N-H···S Geometry[a]

		reduced crystal								
		mol-1			mol-2			oxidized crystal		
D	A	D...A (Å)	H...A (Å)	⟨D−H···A⟩ (deg)	D...A (Å)	H...A (Å)	<D−H...A> (deg)	D...A (Å)	H...A (Å)	⟨D−H···A⟩ (deg)
43N	41Sγ	3.22	2.28	155.6	3.22	2.28	156.7	3.28	2.34	157.1
45Nout	41Sγ	3.40	2.46	155.6	3.35	2.40	153.1			
45Nin	41Sγ	3.40	2.45	159.6	3.38	2.45	158.8	3.39	2.46	154.1
41N	46Sγout	3.83	2.84	169.3	3.83	2.84	168.9			
41N	46Sγin	3.93	2.95	168.9	3.92	2.93	169.7	3.94	2.95	170.0
48Nout	46Sγout	3.34	2.36	166.2	3.38	2.40	167.8			
48Nin	46Sγin	3.39	2.42	164.7	3.43	2.46	164.8	3.40	2.42	166.6
79N	49Sγ	3.49	2.52	163.8	3.48	2.50	164.9	3.55	2.58	164.0
44N	79Sγ	3.51	2.70	138.0	3.47	2.70	134.7	3.54	2.70	141.6
40N	S1	3.27	2.27	171.3	3.21	2.21	171.8	3.28	2.28	178.3
42N	S1	3.30	2.38	153.2	3.30	3.30	155.0	3.29	2.36	154.7
46Nout	S2	3.42	2.58	141.6	3.38	2.50	147.4			
46Nin	S2	3.36	2.43	155.1	3.32	2.38	157.3	3.35	2.44	150.9
47Nout	S2	3.67	2.73	156.5	3.71	2.80	152.3			

[a] D = donor, A = acceptor; in = Cys46-CO pointing toward the cluster and corresponds to the oxidized molecule, out = Cys46-CO pointing away from the cluster and corresponds to the reduced molecule.

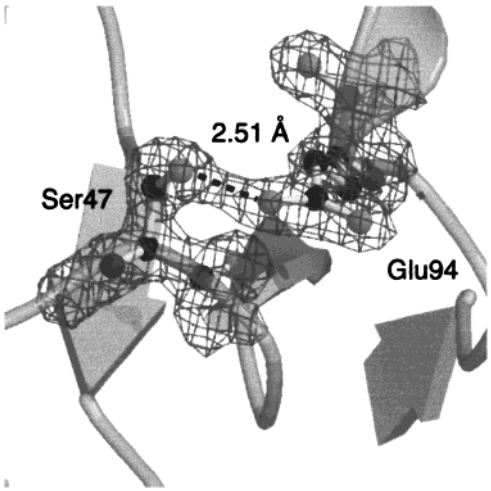

FIGURE 5: Refined model and electron density $2|F_o| - |F_c|$ map (contoured at 1σ) of the Ser47 and Glu94 residues in the oxidized crystal showing a strong hydrogen bond between them. The figure was drawn with BobScript (*51*).

a localized mixed valence Fe^{2+}/Fe^{3+} in the reduced state (*2*). Temperature-dependent proton NMR of the homologous spinach ferredoxin has identified as Fe^{2+} the iron being the closest one to the molecular surface (*33*). Furthermore, due to orbital relaxation, most of the change in net charge upon reduction or oxidation is found to spread over the bridging and terminal cysteine sulfur atoms as shown also on electron density difference maps of a [2Fe−2S] model compound as calculated by density functional theory (DFT) (*34*). As far as the Fd7119 cluster S2 sulfur atom is concerned, an additional negative charge due to reduction will increase the charge dipole repulsion with the negatively charged Cys46 peptide carbonyl oxygen. This could explain why the Cys46−O are pointing away from the cluster S2 sulfur atom for half of the molecules present in the reduced crystal. It is of interest to note that this "CO out" conformation necessarily involves a flip of Ser47−NH, which consequently is pointing toward the cluster S2 atom. This results in an additional charge dipole attraction (NH···S), which also contributes to stabilize the "CO out" conformation. Therefore, we conclude that this "CO out" conformation of Cys46 may be reasonably considered as the signature of the reduced state of the [2Fe−2S] ferredoxin.

By the same criterion, 45−60% of the molecules (i.e., with "CO in") present in the reduced crystals are still oxidized. The reduced crystal was obtained and frozen, at 123 K, under strictly anaerobic conditions, excluding probably further reoxidation. The reduction of only half of the molecules might thus result from an incomplete diffusion of dithionite within the crystal solvent channels. This could also explain why mol-1 is relatively less reduced than mol-2 (40 vs 55%) as its surface neighboring Fe1 is less accessible to solvent, and hence to dithionite, than that of mol-2, due to crystal packing.

It is of interest to note that a redox linked "peptide flip" has also been observed in flavodoxins where, in the semiquinone and reduced forms, a peptide bond changes conformation so that its carbonyl group forms an hydrogen bond with the nearby N5 of the flavin (*35*, *36*). Furthermore, recent analyses of structures and properties of mutants have elegantly shown that this conformational change helps in minimizing the energy of the semiquinone formation and optimizing the flavin interactions with the protein (*37*, *38*).

Cluster Geometry and Its Environment. The present work allows us to have at hand the first precise geometry of a [2Fe−2S] cluster in a protein, based on three independent atomic models, one in the trigonal form and two in the orthorhombic form, which were determined with X-ray data at atomic resolution. The quality of the models is particularly exemplified by the rather small standard deviations (sd's) of the intracluster and cluster−protein interatomic distances (Fe−Fe, S−S, Fe−S, or Fe−Sγ) and angles as derived from block least-squares matrix inversion (Table 4). These sd's are of the same order of magnitude as those obtained for model compounds.

In the oxidized and reduced molecules, the [2Fe−2S] cluster shows a significantly *distorted* D_{2h} symmetry and is definitely non planar as previously detected for a truncated bovine adrenodoxin (*39*) and, to a lesser extent, an analogue (*40*). The Fe−S distances are longer in the S1−Fe1−S2 moiety than in the buried S1−Fe2−S2 moiety. Since the latter moiety shows the same geometry as model compounds

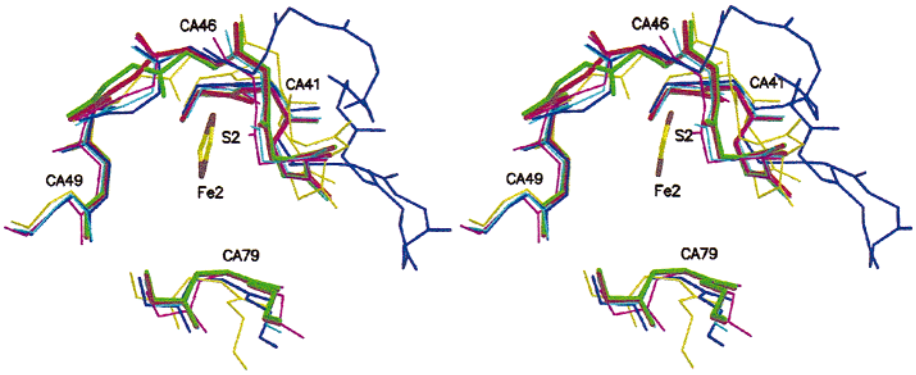

FIGURE 6: Stereoview of the [2Fe−2S] cluster main chain containing a ferredoxin-like domain with conformational variation of the peptide bond centered at Fd7119 Cys46-Ser47. Superposition was performed with the Cα of the four cysteine ligands (rms from 0.07 to 0.4 Å). Main chain of the oxidized and reduced *Anabaena PCC7119* ferredoxin (Fd) are represented in green and red thick lines, respectively. Bovine adrenodoxin (ADX) is drawn with yellow line, *Clostridium pasteurianum* iron−hydrogenase (FEH) with blue line, *Desulfovibrio gigas* aldehyde oxido-reductase (AOR) with cyan line, and *Pseudomonas cepacia* phthalate dioxygenase reductase (PDR) with purple line. The figure was drawn with MolScript (*52*).

(*40*, *41*) (Table 4), this strongly suggests an influence of the protein matrix, e.g. the asymmetric distribution of the NH···S bonds (Table 5 and Figure 4)

Because of the presence within the reduced crystal of a mixture of oxidized and reduced ferredoxins, we took care when comparing the conformations of the oxidized and reduced [2Fe−2S] clusters and their environments. A good indication of the validity and limits of the present results lies in the remarkable similarity between the three oxidized molecules (one in the oxidized crystal and two in the reduced one) on one hand and the two reduced ones on the other hand (Tables 4 and 5). In the reduced ferredoxin molecules, the Fe−S and Fe−Sγ distances tend to be longer than in the oxidized one by, at most, 0.010 Å to 0.020 Å (Table 4), taking into account possible slight displacements of Fe1, Cys46-Sγ, and S2. This increase is lower than those observed for other iron−sulfur proteins (e.g., *42*, *43*). For example, the average increase is 0.04 Å in the *Pyrococcus furiosus* rubredoxin (*44*). This can be explained by the fact that in the oxidized Fd7119 Fe1−S1 and Fe1−S2 are already longer by about 0.05 Å each than Fe2−S1 and Fe2−S2 or the Fe−S distances found in the model compounds. The relative "elongation" of the S1−Fe1−S2 moiety might then help in accommodating the charge density increase due to reduction.

By contrast, the effect of the reduction on the NH···S bond lengths present in the reduced ferredoxin, by comparison with the oxidized one, is more obvious. As expected, the increase of the negative charge on sulfur atoms, upon reduction, strengthens their dipole−dipole interactions with neighboring peptide amide as shown by a significant decrease in the average NH···S bond distances. This is particularly clear for Cys41-NH···Cys46-Sγ (−0.10 Å) and Thr48-NH···Cys46-Sγ (−0.06 Å). The large increase in Cys46-NH···S2 (+0.12 Å) distance is most likely linked with the structural rearrangements associated with the Cys46-O flip (Table 5).

Comparisons with Other [2Fe−2S] Containing Molecules. Superposition of [2Fe−2S] clusters and their environment, found in known [2Fe−2S], containing three-dimensional structures, strikingly shows that the major conformational variation concerns in all cases the peptide bond corresponding to Cys46-Ser47 in *Anabaena* (Figure 6). In adrenodoxin (*39*) and plant-type ferredoxin X-ray structures, the cluster of which is putatively in an oxidized state, the carbonyl oxygen of this peptide oxygen carbonyl is pointing toward the cluster ("CO in") like in the oxidized *Anabaena* ferredoxins.

In the [2Fe−2S] domains of the *Pseudomonas cepacia* phthalate dioxygenase reductase (PDR) (*45*), *Desulfovibrio gigas* xanthine oxidase-related aldehyde oxydoreductase (XOR) (*46*) and *Clostridium pasteurianum* iron hydrogenase (FEH) (*47*), this same carbonyl oxygen is pointing at the opposite side ("CO out") as in the reduced *Anabaena* PCC7119 ferredoxin.

PDR is particularly interesting in that this molecule is a complex including covalently linked FNR and [2Fe−2S] ferredoxin moieties (*45*). Cys277-CO is pointing toward the external medium, whereas Gly278-NH is hydrogen bonded to a cluster sulfur like the corresponding Cys46-CO and Ser47-NH in the reduced ferredoxin from *Anabaena*. Electrostatics (*20*) and density functional theory (*48*) calculations have pointed at a critical role of the protein environment in differentiating the redox potentials of PDR (−174mV) and *Anabaena* PCC7120 ferredoxin (around −400mV). These calculations have shown, in particular, that the PDR Gly278-NH···S* hydrogen bond, accounts for the redox potential shift between the two oxidized proteins. Our present work shows that, in fact, the *Anabaena* ferredoxin undergoes a peptide conformational change on reduction which leads to a cluster protein environment very close to that of the PDR.

In XOR, Cys45-O is making a strong hydrogen bond with Ala136-NH (2.92 Å), which is probably essential for electron transfer between the molybdopterin dinucleotide and the molecular surface (ref *49*, and MJ Romao, personal communication). In FEH, Cys46-O is stabilized by an hydrogen bond with Arg86-Nϵ (3.01 Å).

It should be pointed out that XOR, FEH, and PDR crystal structures have not been determined in their reduced state. This involves that the ("CO out") conformation is not necessarily correlated, as in *Anabaena* Fd, with the nearby [2Fe−2S] cluster reduced state.

Putative FNR Recognition Surface. It is very likely that a prerequisite for electron transfer between ferredoxin and FNR is the formation of a specific complex (*5*, *6*). Several hypothetical models have been proposed, mostly on the basis of the individual FNRs, Fds, and PDR X-ray structures and surface potential calculations (*16*, *19*). They point at a charge and surface complementarity at the complex interface and

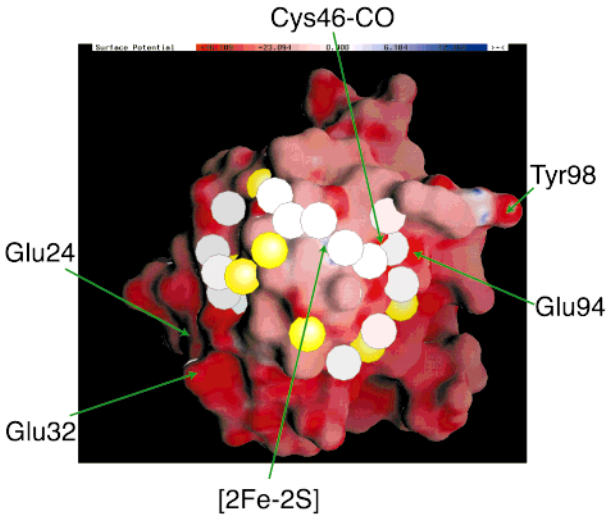

FIGURE 7: Molecular surface drawing of reduced *Anabaena PCC7119* ferredoxin colored according to electrostatic potential (blue, positive; red, negative). Figure is centered on the putative FNR recognition site. Structurally invariant water molecules are represented by yellow circles. Variable water molecules are represented by white circles. The figure was drawn with Grasp (*53*).

close proximity of the Fd [2Fe−2S] cluster to the FNR flavin. Moreover, isothermal calorimetry has shown that the association of Fd and FNR is dominated by a favorable entropy change due, most probably, to the removal of water molecules from the complex interface (*50*). The putative FNR recognition surface of Fd7119 as it appears from the present atomic resolution X-ray studies, qualitatively supports these observations (Figure 7). As earlier mentioned, this surface is delimited by a crown of acidic residues surrounding a nearly hydrophobic zone. It is also covered by water molecules hydrogen bonded to side chains or peptide carbonyl oxygen or amide pointing to the solvent. Ten of them are structurally invariant, since they are located at the same position in the three crystallographic models. This suggests that they are essential in stabilizing the molecular surface. The variable water molecules are more loosely bound to the protein an thus more labile. They might mimick the set of water molecules which are desolvated upon formation of the FNR−Fd complex (*50*).

Site-directed mutagenesis experiments on Fd7120 have pointed at a critical role of Ser47, Phe65, and Glu94 in electron transfer between FNR and ferredoxin (*9*). The present study shows that Ser47 keeps a very similar conformation in the oxidized and reduced ferredoxins. In all cases, Ser47-Oγ is hydrogen bonded to Glu94-Oϵ1. However, in the partialy reduced Fd7119 orthorhombic crystals, whatever the redox state of the molecules, Ser47-Oγ is also hydrogen bonded to the terminal Tyr98-Oη and in close contact with Phe65−Cζ (3.2 Å). It is of interest to note that in the Fd7120 orthorhombic crystal structures (*9*) the terminal Tyr98 of mol-2, although not well-defined, is found to be hydrogen bonded to Ser47-Oγ (OH$\cdots$Oγ = 2.96 Å) and in close contact with Phe65-Cζ (3.9 Å). Along the same lines, the X-ray structure, at 1.4 Å resolution, of the [2Fe−2S] ferredoxin from *Chlorella fusca* (PDB code 1AWD) shows that the terminal Tyr94-Oη is also hydrogen bonded with Ser43-Oη (2.73 Å) and in close contact with Phe61Cζ (3.15 Å). Moreover, in the 2.5 Å X-ray model of the *Spirulina platensis* ferredoxin (ref *16*, PDB code 4FXC) the terminal Tyr98 is also in close contact with Phe65 (3.23 Å) and pointing toward Ser47, but too far to be hydrogen bonded. Altogether, these results show a probable "structural partnership" between Phe65, Ser47, Glu94, and Tyr98. They confirm also the central role of the Ser47 hydroxyl group (*9*), which appears from X-ray studies as a major stabilizing factor of the molecular surface. It should also be mentioned that the Phe65 aromatic ring is nearly stacked onto the 46−47 "flipping" peptide, since the angles between the two planes is about 20 deg and the average interatomic distance 4.2 Å.

The atomic coordinates obtained from the oxidized (code 1QT9) and reduced (code 1CZP) crystals have been deposited at the Protein Data Bank.

ACKNOWLEDGMENT

We are indebted to Carlos Gomez-Moreno for many comments and discussions and his support to this project. We thank Juan Carlos Fontecilla-Camps, Jean Gagnon, and Eric Forest for their interest and support, Jean-Marie Mouesca for suggestions and critical reading of the manuscript, Andrew Thompson and Eric Fanchon for their help in collecting X-ray data at ESRF and Xavier Vernède for his help in the crystal reduction.

REFERENCES

1. Holm, R. H., Kennepohl, P., Solomon, E. I. (1996) *Chem. Rev. 96*, 2239−2314.
2. Beinert, H., Holm, R. H., and Münck, E. (1997) *Science 277*, 653−659.
3. Johnson, M. K. (1998) *Cur. Opin. Chem. Biol. 2*, 173−181.
4. Holden, H. M., Jacobson, B. L., Hurley, J. K., Tollin, G., Oh, B. H., SKjeldahl, L., Chae, Y. K., Cheng, H., Xia, B., and Markley, J. L. (1994) *J. Bioenerg. Biomembr. 26*, 67−88.
5. Foust, G. P., Mayhew, S. G., and Massey, V. (1969) *J. Biol. Chem. 244*, 964−70.
6. Sancho, J., and Gomez-Moreno, C. (1991) *Arch. Biochim. Biophys. 288*, 231−233.
7. Aliverti, A., Deng, Z., Ravasi, D., Piubelli, L., Karplus, P. A., and Zanetti, G. (1998) *J. Biol. Chem. 273*, 34008−34015.
8. Aliverti, A., Livraghi, A., Piubelli, L., and Zanetti, G. (1997) *Biochim. Biophys. Acta 1342*, 45−50.
9. Hurley, J. K., Weber-Main, A. M., Stankovich, M. T., Benning, M. M., Thoden, J. B., Vanhooke, J. L., Holden, H. M., Chae, Y. K., Xia, B., Cheng, H., Markley, J. L., Martinez-Julvez, M., Gomez-Moreno, C., Schmeits, J. L., and Tollin, G. (1997) *Biochemistry 36*, 11100−11117.
10. Martinez-Julvez, M., Medina, M., Hurley, J. K., Hafezi, R., Brodie, T. B., Tollin, G., and Gomez-Moreno, C. (1998) *Biochemistry 37*, 13604−13613.
11. Rypniewski, W. R., Breiter, D. R., Benning, M. M., Wesenberg, G., Oh, B.-H., Markley, J. L., Rayment, I., and Holden, H. M. (1991) *Biochemistry 30*, 4126−4131.
12. Serre, L., Vellieux, F. M., Medina, M., Gomez-Moreno, C., Fontecilla-Camps, J.-C., and Frey, M. (1996) *J. Mol. Biol. 263*, 20−39.
13. Tsukihara, T., Fukuyama, K., Mizushima, M., Harioka, T., Kusunoki, M., Katsube, Y., Hase, T., and Matsubara, H. (1990) *J. Mol. Biol. 216*, 399−410.
14. Jacobson, B. L., Chae, Y. K., Markley, J. L., Rayment, I., and Holden, H. M. (1993) *Biochemistry 32*, 6788−67993.
15. Ikemizu S., Bando M., Sata T., Morimoto Y.,. Tsukihara, T., and Fukuyama, K., (1994) *Acta Crystallogr. D50*, 167−174.
16. Fukuyama, K., Ueki, N., Nakamura, H., Tsukihara, T., and Matsubara, H. (1995) *J. Biochem. (Tokyo) 117*, 1017−1023.
17. Frolow, F., Harel, M., Sussman, J. L., Mevarech, M., and Shoham, M. (1996) *Nat. Struct. Biol. 3*, 452−458.

18. Binda, C., Coda, A., Aliverti, A., Zanetti, G., and Mattevi, A. (1998) *Acta Crystallogr. D Biol. Crystallogr. 54*, 1353−1358.
19. De Pascalis, A. R., Jelesarov, I., Ackermann, F., Koppenol, W. H., Hirasawa, M., Knaff, D. B., and Bosshard, H. R. (1993) *Protein Sci. 2*, 1126−1135.
20. Correll, C. C., Ludwig, M. L., Bruns, C. M., and Karplus, P. A. (1993) *Protein Sci. 2*, 2112−2133.
21. Zhou, J., Hu, Z., Münck, E., and Holm, R. H. (1996) *J. Am. Soc. 118*, 1966−1980.
22. Pueyo, J. J., and Gómez-Moreno, C.(1991) *Prepr. Biochem.* 21, 191−204.
23. Norager, S., Legrand, P., Pieulle, L., Hatchikian, C., and Roth, M. (1999) *J. Mol. Biol. 290*, 881−902.
24. Kabsch, W. (1988) *J. Appl. Crystallogr. 21*, 67−71.
25. Leslie, A. G. W. (1991) in *Molecular Data Processing in Crystallographic Computing* (Moras, D., Podjarny, A. D., and Thierry, J.-C., Eds.) pp 50−61, Oxford University Press.
26. CCP4, Collaborative Computational Project, Number 4. (1994) *Acta Crystallogr. D50*, 760−763.
27. Navaza, J. (1994) *Acta Crystallogr. A50*, 157−163.
28. Jones, T. A., Zou, J. Y., Cowan, S. W., and Kjeldgaard M. (1991) *Acta Crystallogr. A47*, 110−119.
29. Murshudov, G. N., Vagin, A. A., and Dodson, E. J. (1997) *Acta Crystallogr. D53*, 240−255.
30. Lamzin, V, and Wilson, K. (1993) *Acta Crystallogr. D49*, 129−147.
31. Sheldrick, G. M., and Schneider, T. (1997) *Methods Enzymol. 277*, 319−343.
32. Engh, R. A., and Huber, R. (1991) *Acta Crystallogr. A47*, 392−400.
33. Banci, L., Bertini, I., and Luchinat C. (1990) *Struct. Bonding 72*, 113−136.
34. Noodleman, L., Peng, C. Y., Case, D. A., and Mouesca, J.-M. (1995) *Coord. Chem. Rev. 144*, 199−244.
35. Smith, W. W., Burnett, R. M., Darling, G. D., and Ludwig, M. L. (1977) *J. Mol. Biol. 117*, 195−225.
36. W, W., Tulinsky, A., Swenson, R. P., and Watenpaugh, K. D. (1991) *J. Mol. Biol. 218*, 195−208.
37. Ludwig, M. L., Pattridge, K. A., Metzger, A. L., Dixon, M. M., Eren, M., Feng, Y., and Swenson, R. P. (1997) *Biochemistry 36*, 1259−1280.
38. O'Farrell, P. A., Walsh, M. A., McCarthy, A. A., Higgins, T. M., Voordouw, G., and Mayhew, S. G. (1998) *Biochemistry 37*, 8405−8416.
39. Müller, A., Müller, J. J., Muller, Y. A., Uhlmann, H., Bernhardt, R., and Heinemann, U. (1998) *Structure 6*, 269−280.
40. Ueyama, N., Yamada, Y, Okamura, T., Kimura, S., and Nakamura, A. (1996) *Inorg. Chem. 35*, 6473−6484.
41. Mayerle, J. J., Denmark, S. E., De Pamphilis B. V., Ibers, J. A., and Holm, R. H. (1975) *J. Am. Chem. Soc. 97*, 1032−1045.
42. Carter, C. W., Jr., Kraut, J., Freer, S. T., and Alden, R. A. (1974) *J. Biol. Chem. 249*, 6339−6346.
43. Carter, C. W., Jr. (1977) *J. Biol. Chem. 252*, 7802−7811.
44. Day, M. W., Hsu, B. T., Joshua-Tor, L., Park, J. B., Zhou, Z. H., Adams, M. W., and Rees, D. C. (1992) *Protein Sci. 1*, 1494−1507.
45. Correll, C. C., Batie, C. J., Ballou, D. P., and Ludwig, M. L. (1992) *Science 258*, 1604−1610.
46. Romao, M. J., Archer, M., Moura, I., Moura, J. J., LeGall, J., Engh, R., Schneider, M., Hof, P., and Huber, R. (1995) *Science 270*, 1170−1176.
47. Peters, J. W., Lanzilotta, W. N., Lemon, B. J., and Seefeldt, L. C. (1998) *Science 282*, 1853−1858.
48. Li, J., Nelson, M. R., Peng, Ch-Y., Bashford D.; Noodleman L. (1998) *J. Phys. Chem. A 102*, 6311−6324.
49. Romao, M. J., and Huber, R. (1998) *Struct. Bonding 90*, 69−95.
50. Jelesarov, I., and Bosshard, H. R. (1994) *Biochemistry 33*, 13321−13328.
51. Esnouf, R. M. (1997) *J. Mol. Graphics 15*, 133−138.
52. Kraulis, J. P. (1991) *J. Appl. Crystallogr. 24*, 946−950.
53. Nicholls, A., Sharp, K. A., and Honig, B. (1991) *Proteins Struct., Funct., Gen. 11*, 281−296.

BI991578S